Journal of Renewable Materials

Tech Science Press

DOI: 10.32604/jrm.2023.025400 Published Online: 03 November 2022

check for updates

ARTICLE

Study of Thermal, Phase Morphological and Mechanical Properties of Poly(L-lactide)-*b*-Poly(ethylene glycol)-*b*-Poly(L-lactide)/Poly(ethylene glycol) Blend Bioplastics

Yodthong Baimark* **and Theeraphol Phromsopha**

Biodegradable Polymers Research Unit, Department of Chemistry and Centre of Excellence for Innovation in Chemistry, Faculty of Science, Mahasarakham University, Mahasarakham, 44150, Thailand

*Corresponding Author: Yodthong Baimark. Email: yodthong.b@msu.ac.th

Received: 09 July 2022 Accepted: 05 September 2022

ABSTRACT

A poly(L-lactide)-*b*-poly(ethylene glycol)-*b*-poly(L-lactide)(PLLA-PEG-PLLA) block copolymer has great potential for use as a flexible bioplastic. Highly flexible bioplastics are required for flexible packaging applications. In this work, a PEG was incorporated into block copolymer as a plasticizer by solvent casting. PLLA-PEG-PLLA/PEG blends with different blend ratios were prepared, and the plasticizing effect and miscibility of PEG in block copolymer were intensively investigated compared to PLLA/PEG blends. The results indicated that the PEG was an effective plasticizer for the block copolymer. The blending of PEG decreased glass-transition temperature and accelerated the crystallization of both the PLLA and PLLA-PEG-PLLA matrices. The PEG was completely miscible when blended with block copolymer and it improved thermal stability of the block copolymer matrix but not of the PLLA matrix. Film extensibility of PLLA-PEG-PLLA/PEG blends steadily increased as the PEG ratio increased. These non-toxic and highly flexible PLLA-PEG-PLLA/PEG bioplastics are promising candidates for several applications such as biomedical devices, tissue scaffolds and packaging materials.

KEYWORDS

Poly(lactic acid); poly(ethylene glycol); polymer blends; phase morphology; thermal stability

1 Introduction

Poly(L-lactide) or poly(L-lactic acid) (PLLA) has been extensively investigated as an alternative plastic to oil-based plastics in biomedical [1], tissue engineering [2,3] and packaging applications [4]. This is because of its complete biodegradability [5,6], biocompatibility [5,7] and good processability [8–10]. However, the poor flexibility of PLLA with low strain at break (5%−10%) is an important limiting factor restricting its use in many applications [11,12]. A wide variety of plasticizers have been widely blended with PLLA to improve its flexibility by introducing higher chain mobility of PLLA [13,14]. Many factors, such as good miscibility, non-toxicity, plasticizer efficiency, and durability have been considered in the selection of an appropriate plasticizer. Among all plasticizers, poly(ethylene glycol) (PEG) of various molecular weights are highly efficient plasticizers for PLLA, because the PEGs are non-toxic and biocompatible, have good miscibility, and also enhance the hydrolytic degradation ability of PLLA [13–15]. However, phase separation and PEG migration from PLLA matrices have been reported as the main

disadvantage [16–18], which directly affects the stability and durability of the PLLA/PEG blends during storage and applications [19,20].

PLLA-*b*-PEG-*b*-PLLA (PLLA-PEG-PLLA) block copolymers with low molecular weights have been used as macromolecular plasticizers for PLLA [21]. The nucleation and plasticization effects of block copolymers strongly depended on PLLA and PEG block lengths. High-molecular-weight PLLA-PEG-PLLAs were more flexible than PLLA because the PEG blocks act as plasticizers to increase the chain movement of PLLA blocks [22–24]. However, highly flexible PLLA-based bioplastics await development for various applications. In our previous work [25], PLLA was blended with high-molecular-weight PLLA-PEG-PLLA resulting in homogeneous blends. The blending of this block copolymer improved the crystallization ability of the PLLA matrix by both plasticization and nucleation effects.

However, the properties of PLLA-PEG-PLLA/PEG blends have not been reported so far. Although both PEG and PEG-PLLA block copolymers have been investigated for use as effective plasticizers for PLLA, the study of PLLA-PEG-PLLA/PEG blending may lead to the development of novel highly flexible PLLA-based bioplastics. The PEG blocks of the block copolymer are proposed to enhance good miscibility between PLLA blocks and blended PEG. So, in this work, PLLA-PEG-PLLA/PEG blends were prepared by film casting and were compared to PLLA/PEG blends. The phase morphology, crystallization, thermal decomposition, and mechanical properties of blend films were studied.

2 Experiment

2.1 Materials

Synthesis of PLLA and PLLA-PEG-PLLA was accomplished through ring-opening polymerization of L-lactide at 165˚C for 2.5 and 6 h, respectively, referenced in the literature [23–25]. Stannous octoate ($Sn(Oct)_2$, 95%, Sigma) was used as a catalyst. 1-Dodecanol (98%, Fluka) and PEG (molecular weight of 20,000 g/mol, Sigma) were used as initiators for the synthesis of PLLA and block copolymer, respectively. For this purpose, $Sn(Oct)_2$ with concentrations of 0.01 and 0.075 mol% based on the mole of lactide monomer were used for the synthesis of PLLA and block copolymer, respectively. The concentrations of both 1-dodecanol and PEG initiators were 0.144 mol% based on the mole of lactide monomer. The molecular-weight characteristics of the obtained PLLA and block copolymer are summarized in Table 1. PEG (molecular weight of 10,000 g/mol, Fluka) and dichloromethane (99.8% RCI Labscan) were used as blended PEG and solvent, respectively, without further purification.

Table 1: Molecular-weight characteristics of PLLA and PLLA-PEG-PLLA

Sample	Theoretical M_n (g/mol)[a]	$M_{n,GPC}$ (g/mol)[b]	$Đ$[c]
PLLA	100,000	88,400	2.3
PLLA-PEG-PLLA	120,000	89,900	2.8

Notes: [a]Theoretical number-average molecular weight calculated from the monomer/initiator ratio.
[b]Number-average molecular weight obtained from gel permeation chromatography (GPC).
[c]Dispersity index obtained from gel permeation chromatography (GPC).

2.2 Preparation of Blend Films

Blend films were prepared by a solution casting method as follows. PLLA/PEG mixtures (0.6 g) were dissolved completely in dichloromethane (20 mL) before pouring onto a Petri dish and drying at 25°C for 48 h. The obtained blend films were dried in a vacuum oven at 25˚C for 24 h. The 100/0, 95/5, 90/10 and 80/20 (w/w) PLLA/PEG blend films were prepared and investigated. The PLLA-PEG-PLLA/PEG blend films were also fabricated by the same process. The thickness of the obtained film samples was approximately 50 μm.

2.3 Characterization of Blend Films

Attenuated total reflectance-Fourier transform infrared (ATR-FTIR) spectra of the blend films were investigated on a Bruker FTIR spectrometer Invenio-S in the range of 500−3500 cm^{-1} with 30 scans.

Thermal transition properties of the blend films were investigated with a Perkin-Elmer differential scanning calorimeter (DSC) Pyris Diamond under nitrogen flow. The blend films (5−10 mg) were held at 200˚C for 3 min to eliminate the thermal history before fast quenching to 0˚C. The blend films were then heated from 0˚C to 200˚C at a rate of 10 ˚C/min to obtain DSC heating curves. After that, the blend films were scanned from 200˚C to 0˚C at a cooling rate of 10 ˚C/min to obtain DSC cooling curves. The degree of crystallinity (X_c) of the blend films was calculated from enthalpy of melting ($\Delta H_{m,PLLA}$) and enthalpy of cold crystallization (ΔH_{cc}) of PLLA as below.

$$X_c(\%) = [(\Delta H_{m,PLLA} - \Delta H_{cc})/(93 \times W_{PLLA})] \times 100 \quad (1)$$

where the 93 J/g is the ΔH_m for 100%X_c PLLA [26]. The W_{PLLA} is the PLLA weight-fraction of the blend films.

Thermal decompositions of the blend films were investigated on a TA-Instruments thermogravimetric analyzer (TGA) SDT Q600 under nitrogen atmosphere. The blend films were scanned from 50˚C to 600˚C at a heating rate of 20 ˚C/min.

Phase morphologies of the blend films were examined with a JEOL scanning electron microscope (SEM) JSM-6460LV. The blend films were prepared by fracturing after immersing in liquid nitrogen followed by gold sputtered coating before scanning at 20 kV.

The mechanical properties of the blend films were determined on a Liyi universal mechanical testing machine LY-1066B with a gauge length of 50 mm under a strain rate of 50 mm/min. A load cell was 100 kg. At least five measurements for each film were averaged.

3 Results and Discussion

3.1 FTIR

The ATR-FTIR spectra of the blend films are shown in Fig. 1. Pure PLLA film in Fig. 1 (above) showed absorption peaks at 2996 and 2948 cm^{-1} due to the stretching of -CH_3 asymmetric and symmetric, respectively and an absorption peak at 1746 cm^{-1} due to stretching of C=O [13,26]. The absorption peaks at 1181 and 1080 cm^{-1} were C-O-C stretching in ester groups [27,28]. For the PLLA-based blend films, the blended PEG appeared as a broad and multi-shouldered peak at 2882−2883 cm^{-1} attributed to -CH stretching and absorption peaks at 936 and 843 cm^{-1} assigned to -CH_2 rocking [29]. These -CH stretching and -CH_2 rocking peaks of blended PEG significantly increased in intensities as the blended PEG ratio increased.

The pure block copolymer film exhibited the absorption peaks of PLLA blocks identical to those of to the pure PLLA film. A broad peak at 2873 cm^{-1} due to the stretching of -CH of the PEG blocks was also detected [13,29]. As would be expected, the peak intensities of -CH stretching and -CH_2 rocking for the PEG component also increased with the blended PEG ratio. It should be noted that wavenumbers of -CH stretching peaks were 2873, 2890 and 2889 cm^{-1} for 95/5, 90/10 and 80/20 PLLA-PEG-PLLA/PLLA blend films, respectively. Shifting to a higher wavenumber of these peaks as the increasing blended PEG ratio, suggesting that the hydrophobic interactions occurred between the -CH_2 groups of PEG blocks and blended PEG [29].

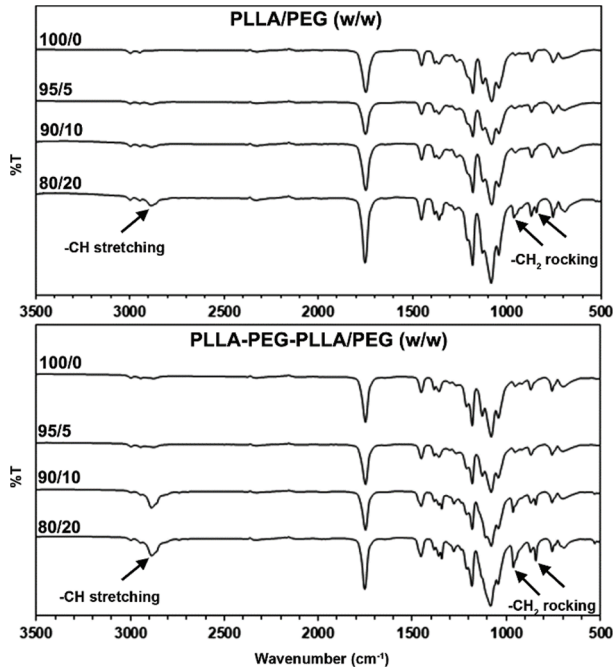

Figure 1: ATR-FTIR spectra of blend films

3.2 Thermal Transition Properties

DSC heating curves of the blend films are presented in Fig. 2 and the DSC results are summarized in Table 2. Fig. 3 shows their expanded T_g and $T_{m,PEG}$ regions. Glass transition temperatures (T_g) of pure PLLA and block copolymer films were 53˚C and 30˚C, respectively. Flexible PEG blocks increased chain mobility of PLLA blocks thereby decreasing its T_g [23,24]. The T_g and cold-crystallization temperatures (T_{cc}) of the PLLA-based blends shifted to the lower temperature as the blended PEG ratio increased. This is explained by the plasticizing effect from blended PEG leading to increased chain movement of the PLLA matrix for the transition from glassy to rubbery and rearrangement of PLLA chains, respectively [17]. The T_g of the block copolymer matrix also shifted to a lower temperature and the T_{cc} peak of the block copolymer disappeared by blending with the PEG, implying that the blending of PEG also enhanced the crystallization of the block copolymer matrix [15]. Degrees of crystallinities (X_c) of both the blend film series increased significantly as the blended PEG ratio increased by plasticization effect, indicating that flexibility of PEG blocks and blended PEG exhibited synergistic effects to improve crystallization properties of PLLA blocks by nucleating and plasticization effects [15].

Melting temperatures of PLLA phases ($T_{m,PLLA}$) for PLLA-based and block copolymer-based blend films were in the ranges 173˚C−176˚C and 169˚C−170˚C, respectively. The $T_{m,PLLA}$ of the PLLA/PEG and PLLA-PEG-PLLA/PEG blend films were shifted to the lowest temperatures at 173˚C and 169˚C, respectively, as the 20%PEG was blended. This may be explained by blended PEG decreasing the surface energy of lamellae overcoming the depression of equilibrium T_m [30]. In addition, the T_m peaks of PEG phases ($T_{m,PEG}$) of the blends were detected for higher blended PEG ratios (20% PEG and 10%PEG for the PLLA-based and block copolymer-based blend films, respectively). The T_m of pure PEG was 66˚C as shown in Fig. 4. This suggests that PEG chains can crystallize in the blends with higher blended PEG ratios [31].

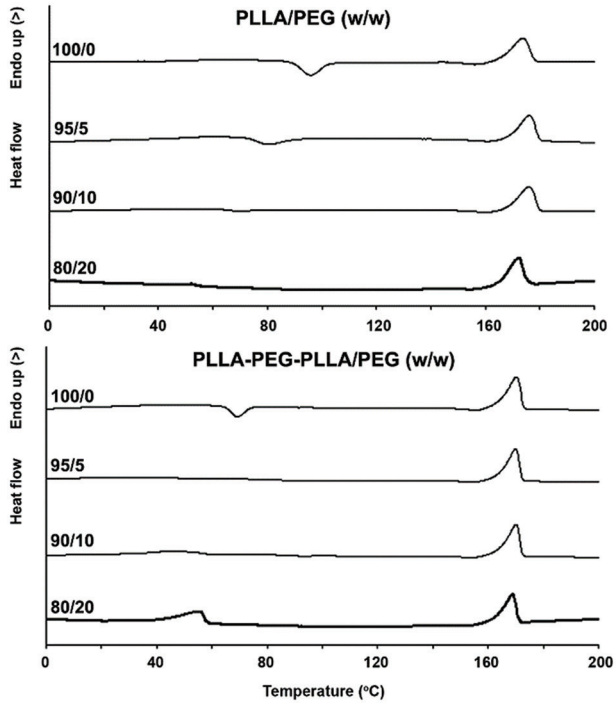

Figure 2: DSC heating curves of blend films

Table 2: Thermal transition properties of blend films from Fig. 2

Film sample	T_g (˚C)	T_{cc} (˚C)	ΔH_{cc} (J/g)	$T_{m,PEG}$ (˚C)	$\Delta H_{m,PEG}$ (J/g)	$T_{m,PLLA}$ (˚C)	$\Delta H_{m,PLLA}$ (J/g)	X_c (%)
PLLA/PEG								
100/0	53	96	29.4	-	-	174	48.4	20.4
95/5	49	80	18.4	-	-	176	44.4	29.4
90/10	-	70	6.3	-	-	176	44.3	45.4
80/20	-	65	1.1	52	3.2	173	46.5	62.5
PLLA-PEG-PLLA/PEG								
100/0	30	69	14.0	-	-	170	45.1	40.3
95/5	23	-	-	-	-	170	43.3	59.1
90/10	-	-	-	46	12.3	170	42.9	61.8
80/20	-	-	-	56	34.6	169	41.1	66.5

Fig. 5 shows the DSC cooling curves of the blend films and the DSC results are reported in Table 3. The pure PLLA and block copolymer films had crystallization temperatures of PLLA phases ($T_{c,PLLA}$) at 105˚C and 108˚C, respectively. The T_c peak at the higher temperature implied faster crystallization [15]. The PEG blocks enhanced the crystallization of PLLA blocks by a plasticizing effect on the DSC cooling scans [22]. The $T_{c,PLLA}$ peaks of both the blend film types shifted to a higher temperature as increasing the blended PEG ratio. Enthalpies of crystallization for PLLA phases ($\Delta H_{c,PLLA}$) were in the ranges 35.9−38.3 J/g and 35.3−36.8 J/g for the PLLA-based and block copolymer-based blend films, respectively.

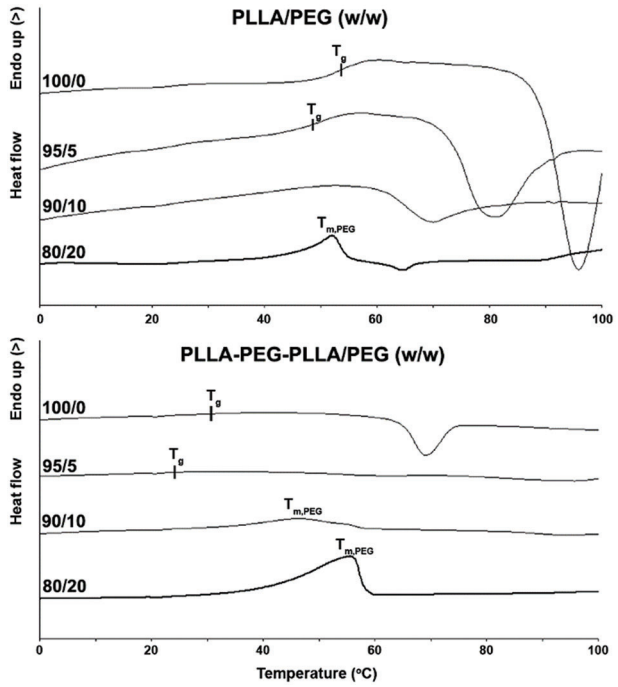

Figure 3: Expanded T_g and $T_{m,PEG}$ regions from Fig. 2 of blend films

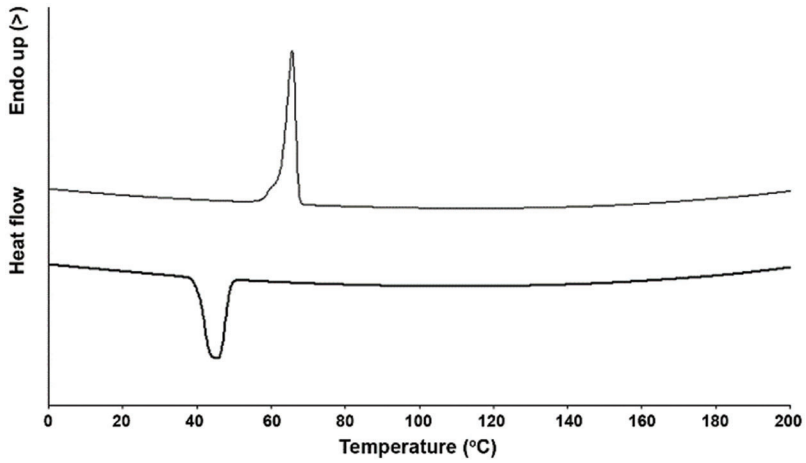

Figure 4: DSC heating (above) and cooling (below) curves of PEG

In addition, $T_{c,PEG}$ peaks appeared in the range 24˚C−40˚C when blended PEG ratios were 20% and 5% for the PLLA-based and block copolymer-based blend films, respectively as summarized in Table 2. The T_c of pure PEG was 45˚C as shown in Fig. 4. The $\Delta H_{c,PEG}$ values of block copolymer-based blend films increased as the blended PEG ratio increased. This may be due to the co-crystallization of PEG blocks and blended PEG.

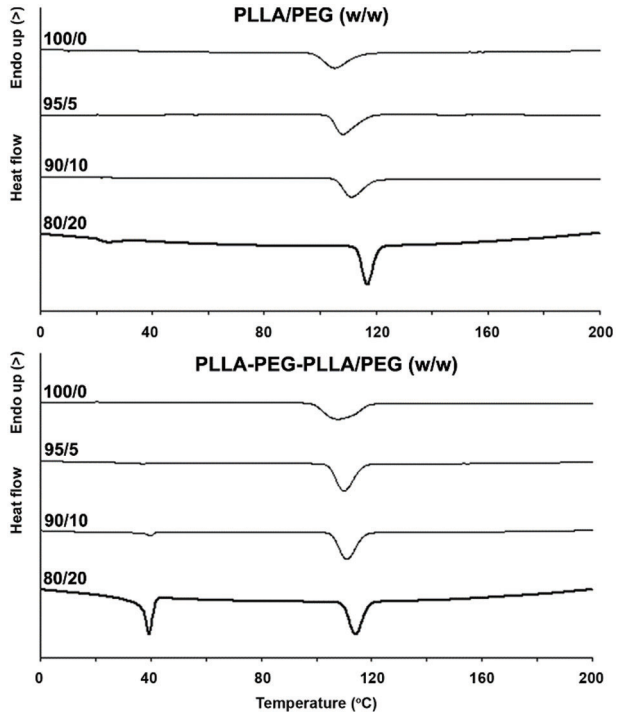

Figure 5: DSC cooling curves of blend films

Table 3: Thermal transition properties of blend films from Fig. 5

Film sample	$T_{c,PEG}$ (˚C)	$\Delta H_{c,PEG}$ (J/g)	$T_{c,PLLA}$ (˚C)	$\Delta H_{c,PLLA}$ (J/g)
PLLA/PEG				
100/0	-	-	105	35.9
95/5	-	-	108	36.5
90/10	-	-	111	36.3
80/20	24	5.1	117	38.3
PLLA-PEG-PLLA/PEG				
100/0	-	-	108	36.8
95/5	37	1.2	110	36.0
90/10	40	3.4	112	36.6
80/20	40	29.5	116	35.3

3.3 Thermal Decompositions

Thermal decompositions of the blend films were investigated from thermogravimetric (TG) curves as illustrated in Fig. 6. Pure PLLA film [Fig. 6 (above, black line)] exhibited a single-step thermal decomposition in the range 300˚C−400˚C due to the "unzipping" mechanism of PLLA chain ends [32]. The TG curves of PLLA-based blend films shifted to lower temperatures as the blended PEG ratio increased. This is expected that blended PEG inhibited interactions of PLLA chains reducing the thermal stability of PLLA matrices [13,33]. The blended PEG fractions had a thermal decomposition in the range of 350˚C−450˚C [23,24]. It can be seen that the contents of blended PEG fractions increased with the blended PEG ratio.

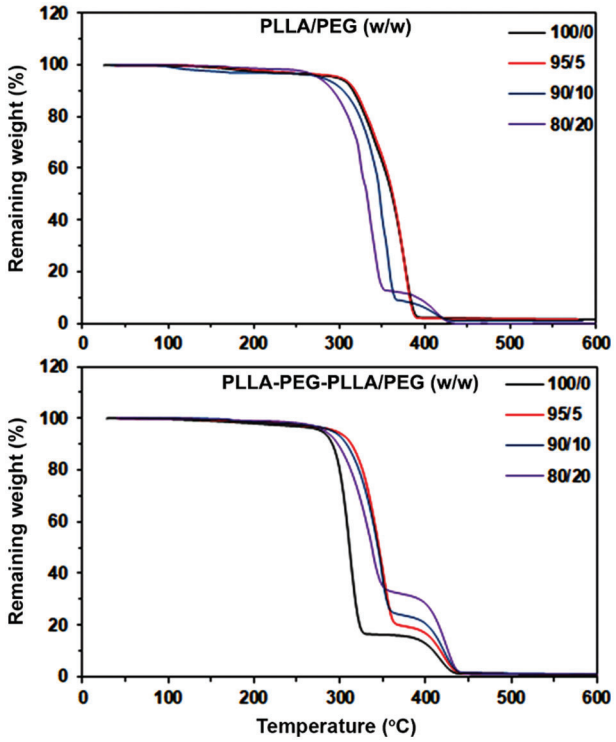

Figure 6: TG curves of blend films

For pure block copolymer film, there was a two-step thermal decomposition of PLLA blocks (250˚C −350˚C) and PEG blocks (350˚C−450˚C) as shown in Fig. 6 (below, black line). The PLLA blocks were more rapidly thermally-decomposed than the pure PLLA due to PEG blocks suppressing interactions of PLLA blocks. It is interesting that the thermal decomposition of PLLA blocks for the block copolymer-based blend films in Fig. 6 (below) was significantly slower than the pure block copolymer film, suggesting that the thermal stability of PLLA blocks of the block copolymer was improved by the addition of blended PEG.

More details on the thermal decompositions of the blend films were studied from derivative TG (DTG) curves, as presented in Fig. 7. A DTG peak was assigned as a maximum decomposition rate temperature ($T_{d,max}$). Table 4 summarizes the $T_{d,max}$ values for all blend films. The pure PLLA film exhibited a $T_{d,max}$ at 366˚C. The $T_{d,max}$ peaks of PLLA-based blend films shifted to a lower temperature when the blended PEG ratio was increased up to 10% (360˚C) and 20% (339˚C). The results supported the view that the blended PEG accelerated the thermal decomposition of the pure PLLA film. This may be due to heterogeneous PLLA and blended PEG interactions replacing homogeneous PLLA and PLLA interactions to provide better PLLA chain movement [33]. The $T_{d,max}$ of blended PEG peaks for PLLA-based blend films appeared when the blended PEG ratios were 10% (410˚C) and 20% (411˚C) suggesting that the blended PEG was aggregated.

The pure block copolymer film had a $T_{d,max}$ of PLLA blocks at 311˚C and a $T_{d,max}$ of PEG blocks at 421˚C. The $T_{d,max}$ peak of PLLA blocks greatly shifted to a higher temperature (349˚C) by blending with 10%PEG. It has been reported that a shielding effect of additives restricted the movement of polymer matrices and gas barrier properties for obstructing the diffusion of decomposition products to improve the thermal stability of polymer matrices [34].

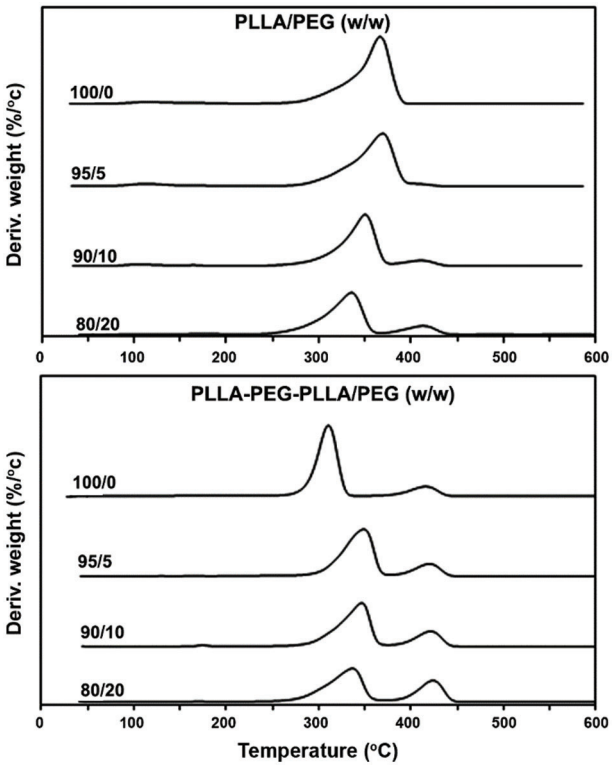

Figure 7: DTG curves of blend films

Table 4: $T_{d,max}$ of blend films from Fig. 7

Film sample	PLLA-$T_{d,max}$ (˚C)	PEG-$T_{d,max}$ (˚C)
PLLA/PEG		
100/0	366	-
95/5	367	-
90/10	360	410
80/20	339	411
PLLA-PEG-PLLA/PEG		
100/0	311	421
95/5	349	421
90/10	348	422
80/20	337	422

3.4 Phase Morphology

SEM images were used to determine the phase morphology of the blend films, as illustrated in Fig. 8. The pure PLLA film had no pores. However, many pores were detected on the PLLA film matrices when the PEG was blended. These pore structures occurred from the infiltration of blended PEG and solvent into bulk PLLA during solvent evaporation [35,36]. Coalescence of these pores was detected for the 80/20 PLLA/PEG blend film [Fig. 8 (left column)].

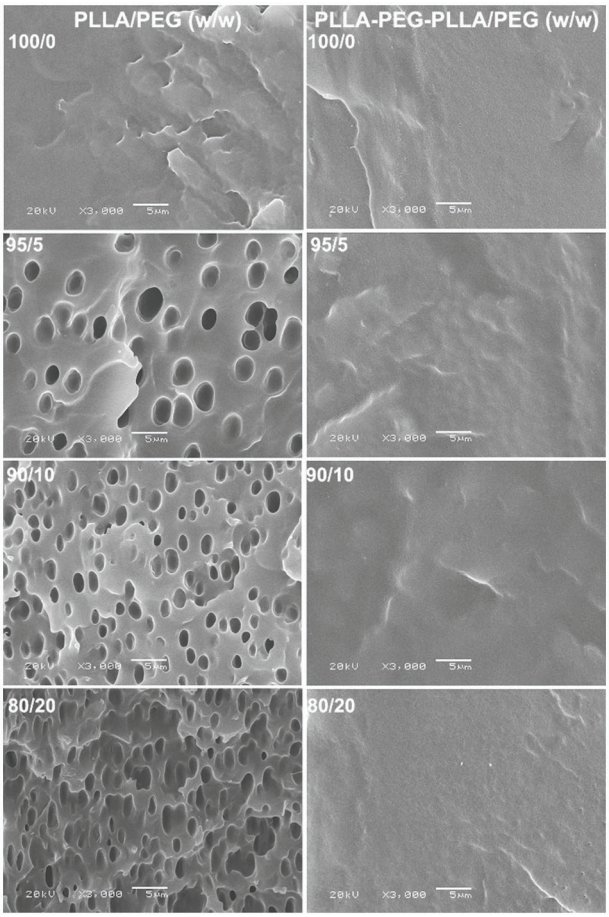

Figure 8: SEM micrographs of fractured surfaces of PLLA/PEG (left column) and PLLA-PEG-PLLA/PEG (right column) blend films

However, the matrices of the block copolymer and its blend films were smoother fracture-surfaces and had no pores as shown in Fig. 8 (right column) indicating that the block copolymer and blended PEG had good phase compatibility. This shows that the PEG blocks enhanced phase compatibility between PLLA blocks and blended PEG.

3.5 Tensile Properties

Fig. 9 shows selected stress-strain curves of the blend films and the tensile properties are reported in Table 5. The pure PLLA film had no yield point because it was highly brittle [11,12]. The PLLA-based blend films exhibited yield points which confirmed that the blended PEG developed PLLA flexibility by decreasing the T_g as described above in DSC results. The yield point phenomenon occurred when stress drops down drastically and is the point at which a sample begins to deform plastically. Stress at yield, stress at break and Young's modulus of PLLA-based blend films decreased but strain at break dramatically increased as the blended PEG ratio increased until the blended PEG ratio was 10%. However, the strain at break of PLLA-based blend films decreased when the blended PEG ratio increased up to 20%. This may be due to larger pores on film matrices decreasing film extensibility during tensile testing [see Fig. 8 (left column)].

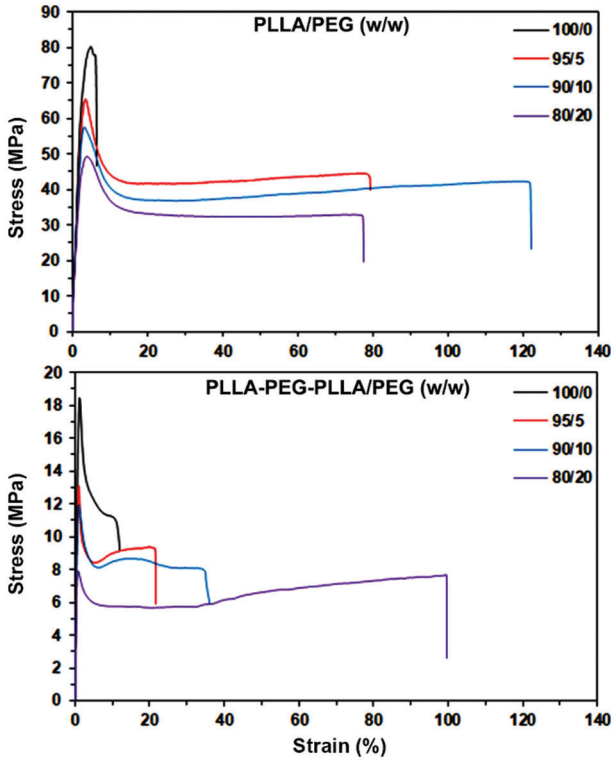

Figure 9: Stress-strain curves of blend films

Table 5: Mechanical properties of blend films from Fig. 9

Film sample	Stress at yield (MPa)	Stress at break (MPa)	Strain at break (%)	Young's modulus (MPa)
PLLA/PEG				
100/0	-	78 ± 6	6 ± 2	1218 ± 34
95/5	69 ± 5	48 ± 5	85 ± 6	937 ± 47
90/10	55 ± 4	44 ± 6	131 ± 9	687 ± 28
80/20	47 ± 6	38 ± 4	76 ± 7	561 ± 31
PLLA-PEG-PLLA/PEG				
100/0	18 ± 4	12 ± 3	14 ± 4	286 ± 28
95/5	14 ± 5	11 ± 4	25 ± 3	225 ± 34
90/10	11 ± 3	8 ± 2	39 ± 5	167 ± 21
80/20	9 ± 2	8 ± 2	105 ± 11	112 ± 23

The pure block copolymer film had a yield point suggesting that it was flexible. The flexible PEG blocks enhanced the flexibility of block copolymer film [23,24]. All the block copolymer-based blend films also exhibited yield points. Stress at yield, stress at break and Young's modulus of block copolymer-based blend films steadily decreased and strain at break increased as the blended PEG ratio increased. The results suggested that the blended PEG in the range of 5%−20% acted as an effective plasticizer for block copolymer film in this study. Good compatibility between block copolymer matrices and blended PEG (5%−20%) was obtained as described in SEM results.

4 Conclusions

In this work, PLLA/PEG and PLLA-PEG-PLLA/PEG blend films were prepared by a solution casting method. The effect of the blended PEG ratio on the properties of blend films was investigated. The blended PEG accelerated crystallization for both the PLLA and block copolymer matrices by a plasticizing effect. The PLLA blocks of the block copolymer-based blend films showed thermal-decomposition at a higher temperature than the pure block copolymer film. The blended PEG improved the thermal stability of the block copolymer matrix but not the PLLA matrix. The block copolymer-based blend films were homogeneous films that indicated good miscibility between block copolymer matrices and blended PEG, whereas, poor miscibility was observed for the PLLA-based blend films. The blended PEG improved film extensibility for both PLLA and block copolymer matrices. The film extensibility of block copolymer-based blends increased steadily as the blended PEG ratio increased. Thus, PLLA-PEG-PLLA/PEG blends could be applied as highly flexible bioplastics. In addition, the PLLA-PEG-PLLA could be used as an effective biodegradable and biocompatible compatibilizer for PLLA/PEG blends that are very promising for biomedical, drug delivery, packaging and agricultural applications.

Acknowledgement: The authors acknowledge the support of the Mahasarakham University and the Center of Excellence for Innovation in Chemistry (PERCH-CIC), Office of the Higher Education Commission, Ministry of Education, Thailand.

Funding Statement: This work was financially supported by Mahasarakham University.

Conflicts of Interest: The authors declare that they have no conflicts of interest to report regarding the present study.

References

1. Kaseem, M., Hamad, K., Ur Rehman, Z. (2019). Review of recent advances in polylactic acid/TiO_2 composites. *Materials, 12(22),* 3659. DOI 10.3390/ma12223659.
2. Majeed, M. H., Kadhem, N. (2022). Morphological evaluation of PLA/soybean oil epoxidized acrylate three-dimensional scaffold in bone tissue engineering. *Journal of Renewable Materials, 10(9),* 2391–2408. DOI 10.32604/jrm.2022.019887.
3. Meng, J., Boschetto, F., Yagi, S., Marin, E., Adachi, T. et al. (2022). Melt-electrowritten poly(L-lactic acid)- and bioglass-reinforced biomimetic hydrogel for bone regeneration. *Materials & Design, 219,* 110781. DOI 10.1016/j.matdes.2022.110781.
4. Brütting, C., Dreier, J., Bonten, C., Altstädt, V., Ruckdäschel, H. (2021). Amorphous polylactide bead foam–effect of talc and chain extension on foaming behavior and compression properties. *Journal of Renewable Materials, 9(11),* 1859–1868. DOI 10.32604/jrm.2021.016244.
5. Lim, L. T., Auras, R., Rubino, M. (2008). Processing technologies for poly(lactic acid). *Progress in Polymer Science, 33(8),* 820–852. DOI 10.1016/j.progpolymsci.2008.05.004.
6. Kaseem, M., Ko, Y. G. (2017). Melt flow behavior and processability of polylactic acid/polystyrene (PLA/PS) polymer blends. *Journal of Polymers and the Environment, 25,* 994–998. DOI 10.1007/s10924-016-0873-5.
7. da Silva, D., Kaduri, M., Poley, M., Adir, O., Krinsky, N. et al. (2018). Biocompatibility, biodegradation and excretion of polylactic acid (PLA) in medical implants and theranostic systems. *Chemical Engineering Journal, 340,* 9–14. DOI 10.1016/j.cej.2018.01.010.
8. Tan, L., Liu, L., Liu, C., Wang, W. (2021). Improvement in the performance of the polylactic acid composites by using deep eutectic solvent treated pulp fiber. *Journal of Renewable Materials, 9(11),* 1897–1911. DOI 10.32604/jrm.2021.016418.
9. Zheng, Y., Xu, M., Tian, J., Yu, M., Tan, B. et al. (2022). Study on the properties of esterified corn starch/Polylactide biodegradable blends. *Journal of Renewable Materials, 10(11),* 2949–2959. DOI 10.32604/jrm.2022.019702.

10. Meng, J., Boschetto, F., Yagi, S., Marin, E., Adachi, T. et al. (2022). Enhancing the bioactivity of melt electrowritten PLLA scaffold by convenient, green, and effective hydrophilic surface modification. *Biomaterials Advances, 135,* 112686. DOI 10.1016/j.msec.2022.112686.
11. Quiles-Carrillo, L., Blanes-Martinez, M. M., Montanes, N., Fenollar, O., Torres-Giner. et al. (2018). Reactive toughening of injection-molded polylactide pieces using maleinized hemp seed oil. *European Polymer Journal, 98,* 402–410. DOI 10.1016/j.eurpolymj.2017.11.039.
12. Jin, F. L., Hu, R. R., Park, S. J. (2019). Improvement of thermal behaviors of biodegradable poly(lactic acid) polymer: A review. *Composites Part B: Engineering, 164,* 287–296. DOI 10.1016/j.compositesb.2018.10.078.
13. Li, D., Jiang, Y., Lv, S., Liu, X., Gu, J. et al. (2018). Preparation of plasticized poly (lactic acid) and its influence on the properties of composite materials. *PLoS One, 13(3),* e0193520. DOI 10.1371/journal.pone.0193520.
14. Greco, A., Ferrari, F. (2021). Thermal behavior of PLA plasticized by commercial and cardanol-derived plasticizers and the effect on the mechanical properties. *Journal of Thermal Analysis and Calorimetry, 146,* 131–141. DOI 10.1007/s10973-020-10403-9.
15. Saeidlou, S., Huneault, M. A., Li, H., Park, C. B. (2012). Poly(lactic acid) crystallization. *Progress in Polymer Science, 37(12),* 1657–1677. DOI 10.1016/j.progpolymsci.2012.07.005.
16. Baiardo, M., Frisoni, G., Scandola, M., Rimelen, M., Lips, D. et al. (2003). Thermal and mechanical properties of plasticized poly(L-lactic acid). *Journal of Applied Polymer Science, 90(7),* 1731–1738. DOI 10.1002/(ISSN) 1097-4628.
17. Kulinski, Z., Piorkowska, E. (2005). Crystallization, structure and properties of plasticized poly(l-lactide). *Polymer, 46(23),* 10290–10300. DOI 10.1016/j.polymer.2005.07.101.
18. Sungsanit, K., Kao, N., Bhattacharya, S. N. (2012). Properties of linear poly(lactic acid)/polyethylene glycol blends. *Polymer Engineering and Science, 52(1),* 108–116. DOI 10.1002/pen.22052.
19. Ma, P., Shen, T., Lin, L., Dong, W., Chen, M. (2017). Cellulose-g-poly(d-lactide) nanohybrids induced significant low melt viscosity and fast crystallization of fully bio-based nanocomposites. *Carbohydrate Polymers, 155,* 498–506. DOI 10.1016/j.carbpol.2016.09.003.
20. Carbonell-Verdu, A., Garcia-Garcia, D., Dominici, F., Torre, L., Sanchez-Nacher, L. et al. (2017). PLA films with improved flexibility properties by using maleinized cottonseed oil. *European Polymer Journal, 91,* 248–259. DOI 10.1016/j.eurpolymj.2017.04.013.
21. Li, L., Cao, Z. Q., Bao, R. Y., Xie, B. H., Yang, M. B. et al. (2017). Poly(L-lactic acid)-polyethylene glycol-poly(L-lactic acid) triblock copolymer: A novel macromolecular plasticizer to enhance the crystallization of poly(L-lactic acid). *European Polymer Journal, 97,* 272–281. DOI 10.1016/j.eurpolymj.2017.10.025.
22. Yun, X., Li, X., Jin, Y., Sun, W., Dong, T. (2018). Fast crystallization and toughening of poly(L-lactic acid) by incorporating with poly(ethylene glycol) as a middle block chain. *Polymer Science. Series A, 60,* 141–155. DOI 10.1134/S0965545X18020141.
23. Baimark, Y., Rungseesantivanon, W., Prakymoramas, N. (2018). Improvement in melt flow property and flexibility of poly(L-lactide)-*b*-poly(ethylene glycol)-*b*-poly(L-lactide) by chain extension reaction for potential use as flexible bioplastics. *Materials & Design, 154,* 73–80. DOI 10.1016/j.matdes.2018.05.028.
24. Baimark, Y., Srisuwan, Y. (2020). Thermal and mechanical properties of highly flexible poly(L-lactide)-*b*-poly (ethylene glycol)-*b*-poly(L-lactide) bioplastics: Effects of poly(ethylene glycol) block length and chain extender. *Journal of Elastomers & Plastics, 52(2),* 142–158. DOI 10.1177/0095244319827993.
25. Baimark, Y., Rungseesantivanon, W., Prakymoramas, N. (2021). Crystallization and toughness of poly(L-lactide) by melt blending with poly(L-lactide)-b-polyethylene glycol-b-poly(L-lactide) in the presence of chain extender. *Polymer Science, Series A, 63,* S34−S45. DOI 10.1134/S0965545X22030051.
26. Szefer, E., Leszczyńska, A., Hebda, E., Pielichowski, K. (2021). The application of cellulose nanocrystals modified with succinic anhydride under the microwave irradiation for preparation of polylactic acid nanocomposites. *Journal of Renewable Materials, 9(6),* 1127–1142. DOI 10.32604/jrm.2021.014584.
27. Ferrarezi, M. M. F., de Oliveira Taipina, M., da Silva, L. C. E., Goncalves, M. C. (2013). Poly(ethylene glycol) as a compatibilizer for poly(lactic acid)/thermoplastic starch blends. *Journal of Polymers and the Environment, 21,* 151–159. DOI 10.1007/s10924-012-0480-z.

28. Cuevas-Carballo, Z. B., Duarte-Aranda, S., Canch´e-Escamilla, G. (2019). Properties and biodegradation of thermoplastic starch obtained from grafted starches with poly(lactic acid). *Journal of Polymers and the Environment, 27,* 2607–2617. DOI 10.1007/s10924-019-01540-w.
29. Özdemir Dinç, C., Güner, A. (2017). Solid-state characterization of poly(ethylene glycol) samples prepared by solvent cast technique. *Bulgarian Chemical Communications, 49,* 15–20.
30. Lai, W. C., Liau, W. B., Lin, T. T. (2004). The effect of end groups of PEG on the crystallization behaviors of binary crystalline polymer blends PEG/PLLA. *Polymer, 45,* 3073–3080. DOI 10.1016/j.polymer.2004.03.003.
31. Li, F. J., Zhang, S. D., Liang, J. Z., Wang, J. Z. (2015). Effect of polyethylene glycol on the crystallization and impact properties of polylactide-based blends. *Polymers for Advanced Technologies, 26(5),* 465–475. DOI 10.1002/pat.3475.
32. Mothe, C. G., Azevedo, A. D., Drumond, W. S., Wang, S. H. (2010). Thermal properties of amphiphilic biodegradable triblock copolymer of L,L-lactide and ethylene glycol. *Journal of Thermal Analysis and Calorimetry, 101,* 229–233. DOI 10.1007/s10973-009-0589-z.
33. Mohapatra, A. K., Mohanty, S., Nayak, S. K. (2014). Effect of PEG on PLA/PEG blend and its nanocomposites: A study of thermo-mechanical and morphological characterization. *Polymer Composites, 35(2),* 283–293. DOI 10.1002/pc.22660.
34. Shen, W., Wu, W., Liu, C., Wang, Z., Huang, Z. (2020). Achieving a high thermal conductivity for segregated BN/PLA composites via hydrogen bonding regulation through cellulose network. *Polymers for Advanced Technologies, 31(9),* 1911–1920. DOI 10.1002/pat.4916.
35. Chen, B. Y., Wang, Y. S., Mi, H. Y., Yu, P., Kuang, T. R. et al. (2014). Effect of poly(ethylene glycol) on the properties and foaming behavior of macroporous poly(lactic acid)/sodium chloride scaffold. *Journal of Applied Polymer Science, 131(23),* 41181. DOI 10.1002/app.41181.
36. Darabian, B., Bagheri, H., Mohammadi, S. (2020). Improvement in mechanical properties and biodegradability of PLA using poly(ethylene glycol) and triacetin for antibacterial wound dressing applications. *Progress in Biomaterials, 9,* 45–64. DOI 10.1007/s40204-020-00131-6.